FUDMA Journal of Sciences (FJS)
ISSN online: 2616-1370
ISSN print: 2645 - 2944
Vol. 9 No. 5, May, 2025, pp 87 - 96
DOI: https://doi.org/10.33003/fjs-2025-0905-3588

ASSESSMENT OF NATURAL RADIOACTIVITY AND RADIOLOGICAL RISKS IN SOIL OF NUMBUPI MINING SITE IN NIGER STATE, NIGERIA: PUBLIC HEALTH AND ENVIRONMENTAL IMPLICATIONS

***[1]Musa Jibril, [1]Abdulsalam Shehu, [2]Aregbe O. Olubunmi, [3]Abdullahi A. Abubakar, [1]Nuraddeen N. Garba, [4]Usman Adamu, [1]Aliyu Muhammad, [5]Abdulkadir Mukhtar, [1]Abdullahi M. Vatsa, [1]Usman M. Kankara and [6]Yamusa A. Yamusa**

[1]Department of Physics, Ahmadu Bello University, Zaria
[2]Department of Physics and Astronomy, University of Minnesota, USA
[3]Deparment of Radiotherapy and Oncology, Ahmadu Bello University, Teaching Hospital, Shika, Zaria
[4]Department of Physics, Faculty of Physical Sciences, Kaduna State University, Kaduna State, Nigeria
[5]Department of General Studies, Federal University of Transportation, Daura. Katsina State
[6]Center for Energy Research and Training, Ahmadu Bello University, Zaria

*Corresponding authors' email: mjibril2022@gmail.com

ABSTRACT

The study was conducted in Numbupi, a gold-mining settlement in Chanchaga Local Government Area, Niger State, Nigeria. The area features lowland topography surrounded by rock formations and is characterized by open-pit mining practices. The study uses gamma spectrometry with a sodium iodide (NaI (Tl)) detector to assess the natural radioactivity concentrations of ^{226}Ra, ^{232}Th, and ^{40}K in seven soil samples collected from the Numbupi Mining Site in Niger State, Nigeria. The mean activity concentrations of ^{226}Ra (85.81 ± 18.32 Bq/kg), ^{232}Th (15.84 ± 8.21 Bq/kg), and ^{40}K (213.41 ± 89.67 Bq/kg) were calculated and compared with world mean values. A high ^{40}K concentration in Sample 5 (324.45 Bq/kg) is likely driven by anthropogenic sources, potassium fertilizer application, as it is a well-documented contributor to ^{40}K enrichment, and natural (alluvial) interactions, while elevated ^{226}Ra concentration in Samples 1 (136.70 Bq/kg) and 7 (120.72 Bq/kg) correlated with local granitic geology. The following radiological health parameters were calculated: radium equivalent activity (124.90 ± 42.56 Bq/kg), absorbed dose rate (58.11 ± 18.23 nGy/h), annual effective dose equivalent (0.36 ± 0.12 mSv/y), and hazard indices (H_{ex} = 0.34 ± 0.12, H_{in} = 0.57 ± 0.22). The observed correlations between natural radionuclides (^{226}Ra, ^{232}Th, and ^{40}K) in the analyzed soil samples reflect complex geological and anthropogenic interactions. The study revealed a strong positive correlation between ^{232}Th and ^{40}K (r = +0.85), primarily driven by Samples 5 and 7, indicating that soils with higher thorium concentrations also tend to have elevated potassium levels. All the calculated values were found to be well below international safety thresholds, confirming minimal radiological risks to the public. The study suggests routine monitoring that mitigates long-term exposure hazards and emphasizes the significance of site-specific radiological assessments for ensuring environmental safety.

Keywords: Soil contamination, Natural radioactivity, Radiological hazards, Gamma spectrometry, Dose assessment, Hazard index

INTRODUCTION

In terrestrial contexts, natural radionuclides such as potassium (^{40}K), uranium (^{238}U), and thorium (^{232}Th) are common and account for around 80% of human exposure to ionizing radiation (El-Taher and Elsaman, 2018). According to Tzortzis and Tsertos (2004), these radionuclides decay, producing progeny like ^{226}Ra (from the ^{238}U family) and ^{220}Rn (from ^{232}Th), which release gamma radiation and are potentially hazardous when inhaled. While global averages for soil radioactivity are well-established (e.g., 32 Bq/kg for ^{226}Ra, 45 Bq/kg for ^{232}Th, and 420 Bq/kg for ^{40}K) (UNSCEAR, 2000), localized geological and anthropogenic factors can elevate concentrations, necessitating region-specific evaluations. However, recent studies highlight the role of mining, fertilizer usage, and industrial activities in altering natural radionuclide distributions (Ghiassi-Nejad *et. al.*, 2002; Faweya *et. al.*, 2023). Phosphate fertilizers, for example, raise ^{226}Ra activity in agricultural soils (ICRP, 2007), and granite-rich terrains increase ^{232}Th concentrations (Musthafa and Krishnan, 2017). Long-term exposure to such conditions raises the chance of developing cancer, especially if radon gas (^{222}Rn) is inhaled (Rahman, 2020).

Artisanal and small-scale mining (ASM) activities, particularly in developing nations, represent a critical anthropogenic factor influencing radionuclide distribution. Open-pit mining disrupts soil strata, mobilizes uranium- and thorium-bearing minerals, and amplifies dust-borne radionuclide dispersion. Despite their economic importance, such activities are rarely accompanied by radiological risk assessments, leaving communities vulnerable to undocumented exposure (ILO, 2022; Usman *et. al.*, 2022).

This study focuses on Numbupi, a mining settlement in Chanchaga Local Government Area, Niger State, Nigeria. The region is characterized by lowland terrain with granitic bedrock and is accessible only via rugged, unpaved pathways. Numbupi's economy revolves around artisanal open-pit mining, which employs rudimentary techniques to extract ore from shallow pits. The mining process generates fine particulate matter, which may entrain uranium-series radionuclides (e.g., ^{226}Ra) and thorium-bearing minerals, elevating inhalation risks for miners and nearby residents. Furthermore, subsistence farming in adjacent areas introduces potassium-rich fertilizers, potentially altering ^{40}K soil concentrations (Mansur and Sunusi, 2020). Despite global data, region-specific studies in under-resourced mining areas like Numbupi remain scarce. Therefore, to fill important gaps in radiological data for understudied areas, this study quantifies ^{226}Ra, ^{232}Th, and ^{40}K concentrations in surface soils, calculates the radiological health parameters (Absorbed Dose Rate (D), Annual Effective Dose Equivalent (AEDE),

Radium Equivalent Activity (Ra_{eq}), Hazard Indices (H_{ex}, H_{in}) and Gamma Index (I_{γ})), and benchmarks the results against international safety standards (IAEA, 2014 and UNSCEAR, 2000).

MATERIALS AND METHODS

Materials

Soil samples preparation for the detection of natural radionuclides was achieved with the use of plastic container, candle wax, masking tape, hand gloves, analytical wind balance, Geiger counter radiation detector (GQ GMC-500+), and NaI(TI) (detector model 727 series, Canberra Inc.).

Study Area

The study was conducted in Numbupi, a gold-mining settlement in Chanchaga Local Government Area, Niger State, Nigeria. The mid-point of the mining site is given by latitude 9^0 34'35"N and longitude $6^0$35'30"E (Plate 1). The terrain is rugged and rocky, accessible only by motorbike, with no formal roads. The area features lowland topography surrounded by rock formations and is characterized by open-pit mining practices. Post-mining land abandonment has led to vegetation destruction and significant topographic alteration. Local livelihoods rely on subsistence farming and artisanal gold mining.

Plate 1: Satellite image of the study area with sample collection points

Sample Collection and Preparation

Sampling

Seven soil samples were collected from abandoned mining pits and adjacent areas using clean plastic containers to avoid cross-contamination. Samples were labelled systematically and transported to the Centre for Energy Research and Training (CERT), Ahmadu Bello University, Zaria, for analysis.

Preparation

Drying: Samples were air-dried at ambient temperature until constant mass was achieved.

Homogenization: Dried soils were pulverized using a mortar and pestle, then sieved through a 2 mm mesh to remove debris.

Sealing: Due to detector constraints, 200 – 300 g of each homogenized sample were transferred to radon-impermeable cylindrical plastic containers (66 mm height × 65 mm diameter). Containers were sealed with candle wax and masking tape to prevent radon leakage and stored for 28 days to establish secular equilibrium between ^{226}Ra and its decay products, justified by the principles of radioactive decay dynamics and practical radiochemical requirements **(IAEA,** 1989).

Instrumentation

Gamma spectrometry was performed using a 76 × 76 mm NaI(Tl) scintillation detector (Model 727 series, Canberra Inc.) coupled to a Canberra Series 10 Plus Multichannel Analyzer (MCA) (Model 1104). Key specifications:

Energy Resolution: 8% at 662 keV (^{137}Cs).

Peak Selection: ^{226}Ra (via ^{214}Bi at 1760 keV), ^{232}Th (via ^{208}Tl at 2615 keV) and ^{40}K (via 1460 keV γ-ray).

A Geiger-Müller counter (GQ GMC-500+) (Plate 2) was used for preliminary field radiation screening.

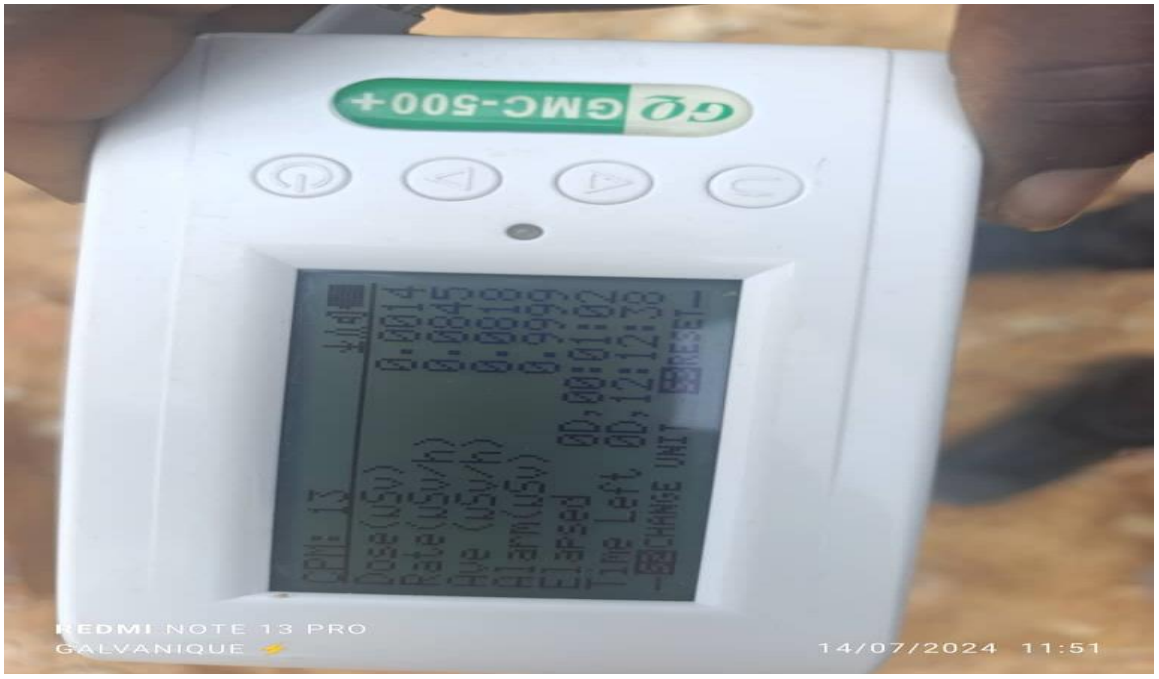

Plate 2: Geiger-Müller counter (GQ GMC-500+) used for initial radiation screening

Radioactivity Measurement

Calibration

The detector was energy-calibrated using ^{137}Cs (662 keV) and ^{60}Co (1332 keV).

Counting

Samples were placed symmetrically on the detector and counted for 29,000 seconds (8 hours) to ensure statistical precision.

Background Subtraction

Background spectra (empty container) were acquired and subtracted from sample counts to isolate net peak areas.

Data Analysis

The following formulas were used to compute radiological parameters and statistical correlations:

Activity Concentration

To quantify the specific radioactivity of ^{226}Ra, ^{232}Th, and ^{40}K in soil samples (in Becquerel per kilogram, Bq/kg), net gamma-ray counts were normalized to detector efficiency, counting time, and sample mass:

$$A(Bq/kg) = \frac{N}{\varepsilon \times t \times m} \quad (1)$$

where:

N: Net counts under the gamma-ray peak.

ε: Detector efficiency at the specific energy.

t: Counting time (seconds).

m: Mass of the sample (kg).

Radiological Hazard Parameters

Absorbed Dose Rate (D)

To estimate the total gamma radiation dose rate in air (nGy/h) from terrestrial radionuclides, weighted contributions of ^{226}Ra, ^{232}Th, and ^{40}K were summed using UNSCEAR (2000) coefficients:

$$D(nGy/h) = 0.462A_{Ra} + 0.604A_{Th} + 0.0417A_K \quad (2)$$

Coefficients 0.462, 0.604 and 0.0417 represent conversion factors for gamma-ray contributions from ^{226}Ra, ^{232}Th, and ^{40}K (UNSCEAR, 2000). A_{Ra}, A_{Th}, and A_K represent activity concentrations of ^{226}Ra, ^{232}Th, and ^{40}K (Bq/kg) respectively.

Annual Effective Dose Equivalent (AEDE)

To evaluate long-term radiation exposure risks to the public (mSv/y), the absorbed dose rate was scaled by outdoor occupancy (70%) and annual exposure duration:

$$AEDE(mSv/y) = D \times 0.7\ (\text{occupancy factor}) \times 8760\ h/y \times 10^{-6} \quad (3)$$

Radium Equivalent Activity (Ra_{eq})

To assess the combined gamma radiation impact of ^{226}Ra, ^{232}Th, and ^{40}K relative to radium-226, their activities were weighted by dose conversion factors (Beretka & Mathew, 1985):

$$Ra_{eq}(Bq/kg) = A_{Ra} + 1.43A_{Th} + 0.077A_k \quad (4)$$

Normalizes combined radiological effects to ^{226}Ra (Beretka & Mathew, 1985).

Hazard Indices

To determine the safety of soils for construction or agricultural use, external (H_{ex}) and internal (H_{in}) hazard indices were calculated:

External Hazard Index (H_{ex})

Reflects gamma radiation risks:

$$H_{ex} = \frac{A_{Ra}}{370} + \frac{A_{Th}}{259} + \frac{A_K}{4810} \quad (5)$$

Internal Hazard Index (H_{in})

Accounts for radon gas inhalation risks:

$$H_{in} = \frac{A_{Ra}}{185} + \frac{A_{Th}}{259} + \frac{A_K}{4810} \quad (6)$$

Gamma Index (I_γ)

To comply with EU safety standards for building materials (European Council, 2013), the gamma index normalizes combined radiological effects to a threshold of 1:

$$H_{ex} = \frac{A_{Ra}}{300} + \frac{A_{Th}}{200} + \frac{A_K}{3000} \quad (7)$$

Threshold: $I_\gamma \leq 1$ (European Council, 2013).

Pearson's Correlation Coefficient (r)

To quantify linear relationships between radionuclide pairs (e.g., ^{226}Ra and ^{232}Th), covariance was scaled by the product of standard deviations:

$$r = \frac{\sum(x_i-\bar{x})(y_i-\bar{y})}{\sqrt{\sum(x_i-\bar{x})^2 \sum(y_i-\bar{y})^2}} \quad (8)$$

where x_i and y_i represent activity concentrations of two radionuclides.

RESULTS AND DISCUSSION

The results of this study provide critical insights into the natural radioactivity levels and associated radiological risks in the analyzed soil samples.

Background Radiation Levels

In-situ radiation levels were preliminarily assessed using a Geiger-Müller counter (GQ GMC-500+). Measurements were taken at seven points across the mining site (Table 1), An Accumulated Dose (µSv) which is the total radiation exposure per point and the Dose Rate (µSv/h) which is the instantaneous radiation intensity were recorded. Background readings were compared to the global mean average external exposure to natural terrestrial radiation sources value of 0.48 mSv/y (UNCEAR, 2008).

Table 1: Background Radiation Levels at Numbupi Mining Site

Sample Point	Accumulated Dose (µSv)	Dose Rate (µSv/h)
1	0.0018	0.1105
2	0.0021	0.1170
3	0.0017	0.1040
4	0.0022	0.1800
5	0.0026	0.1495
6	0.0025	0.1560
7	0.0017	0.1105
Mean	0.0021	0.1320
Safety Limit	–	≤ 0.1

The background dose rates at Numbupi mining site ranged from 0.1040 µSv/h (Point 3) to 0.1800 µSv/h (Point 4), with a mean of 0.1320 µSv/h (Table 1). These values exceed the global outdoor average of 0.07 µSv/h (UNSCEAR, 2000) and the recommended limit of ≤ 0.1 µSv/h for non-mining areas, likely due to:

Mining Activities: Disturbance of uranium-bearing minerals (e.g., granite) releasing ^{226}Ra and ^{222}Rn.

Soil Heterogeneity: Elevated ^{232}Th in Points 4 – 6 (dose rate: 0.1495 – 0.1800 µSv/h) aligns with heavy mineral deposits (e.g., monazite).

Correlation with Soil Activity Concentrations

The highest dose rate (0.1800 µSv/h) corresponds to Sample 4 in soil analysis, which showed that ^{226}Ra (90.54 Bq/kg) and ^{40}K (205.77 Bq/kg) are the major contributors to the radiation dose level at the point. This consistency validates the use of field (Geiger counter) for preliminary environmental radiation dose measurement for radiological risk assessment.

Activity Concentrations of Radionuclides

The radiological analysis of soil samples from the study area revealed concentrations of natural radionuclides (^{226}Ra, ^{232}Th, and ^{40}K) and associated health parameters within globally accepted safety limits (Table 2). The table interprets the findings in the context of geological influences, public health implications, and global benchmarks, supported by comparisons to existing literature.

Table 2: Radiological Analysis of Soil Samples (with Safety Limits)

Sample ID	Concentration of Natural Radionuclide (BQ/KG)			Absorbed Dose Rate (D)	AEDE	RA_{EQ}	H_{EX}	H_{IN}	I_Γ
	^{226}Ra	^{232}Th	^{40}K						
1	136.70	9.76	232.86	78.75	0.48	168.59	0.46	0.83	0.58
2	131.90	6.61	83.82	68.43	0.42	147.80	0.40	0.76	0.50
3	22.28	13.06	193.92	26.26	0.16	55.88	0.15	0.21	0.20
4	90.54	10.58	205.77	56.80	0.35	121.51	0.33	0.57	0.42
5	18.10	30.20	324.45	40.13	0.25	86.29	0.23	0.28	0.32
6	80.43	12.26	150.49	50.83	0.31	109.55	0.30	0.51	0.38
7	120.72	28.42	302.56	85.54	0.52	184.67	0.50	0.83	0.65
Mean	85.81	15.84	213.41	58.11	0.36	124.90	0.34	0.57	0.44
Safety limit	32	45	420	≤ 59	≤ 0.48	≤ 370	≤ 1	≤ 1	≤ 1

The mean ^{226}Ra concentration (85.81 Bq/kg) exceeds the global average (32 Bq/kg) reported by UNSCEAR, 2000, but remains 4.3 times lower than the IAEA safety limit (370 Bq/kg) (IAEA, 2014). Elevated ^{226}Ra in Samples 1 (136.70 Bq/kg) and 7 (120.72 Bq/kg) correlates with the region's granitic bedrock, which often contains uranium-bearing minerals like pitchblende and autunite (Kumar *et al.,* 2019). Similar enrichments have been observed in granite-rich terrains of India (Kumar *et. al.,* 2019) and Brazil (Veiga *et. al.,* 2006). The absence of anthropogenic uranium sources (e.g., mining or nuclear waste) suggests natural geological processes dominate ^{226}Ra distribution. However, Esan *et al.* (2022) measured mean value of 11.19 Bq/kg in Ile-Ife soils

which is well below both world average and Numbupi mean value of 85.81 Bq/kg.

The low ^{232}Th concentration (15.84 Bq/kg) is 65% lower than the global average (45 Bq/kg) (Tzortzis and Tsertos, 2004), reflecting the scarcity of thorium-rich minerals (e.g., monazite, thorite) in the study area. This aligns with findings from alluvial plains in Bangladesh (Rahman *et al.,* 2020), where ^{232}Th levels were similarly subdued due to sedimentary dilution (Almayahi *et. al.,* 2012). Sample 5 (30.20 Bq/kg) represents an outlier, possibly linked to minor zircon or ilmenite deposits in agricultural soils (Taskin *et al.,* 2009). However, Abdulmalik *et al.* (2024) reported a mean value of 8.8 Bq/kg in swampy Nasarawa farmlands, Nigeria but ~ 44% lower than the Numbupi soils mean value of 15.84 Bq/kg.

The mean ^{40}K activity (213.41 Bq/kg) is 49% lower than the global average (420 Bq/kg) (Tzortzis, and Tsertos, 2004), but Sample 5 (324.45 Bq/kg) approaches this benchmark. Elevated ^{40}K in agricultural soils (Sample 5) likely stems from potassium fertilizer application, a well-documented contributor to ^{40}K enrichment (Taskin *et. al.,* 2009). Conversely, low ^{40}K in Sample 2 (83.82 Bq/kg) may reflect leaching in waterlogged soils, as observed in tropical deltaic regions (Almayahi *et. al.,* 2012). In addition, Abdulmalik *et al.* (2024) found extremely high ^{40}K (875.5 Bq/kg) in Kokona swamp soils of Nigeria, driven by organic-rich sediments, more than 4 times the 213.41 Bq/kg reported in this study and underscoring the variability among Nigerian environments.

Radiological Health Parameters

Absorbed Dose Rate

The mean absorbed dose rate (58.11 nGy/h) is slightly lower than the global average 59 nGy/h set by UNSCEAR (UNSCEAR, 2000; Tzortzis, and Tsertos, 2004). The highest dose rate (Sample 7: 85.54 nGy/h) remains within safe margins. These values are comparable to doses reported in uncontaminated soils of Turkey (Karahan *et al.,* 2020) but lower than those in phosphate-mining regions of Egypt (Karahan *et. al.,* 2020; Ghiassi-Nejad, *et. al.,* 2002).

Annual Effective Dose Equivalent

The mean AEDE (0.36 mSv/y) is 75% lower than the world mean of 0.48 mSv/y for normal natural background exposure (UNCEAR, 2000), confirming minimal risk to residents. Even the highest individual AEDE (Sample 7: 0.52 mSv/y) represents just 1.08% above the limit, contrasting sharply with high-background radiation areas (HBRAs) like Ramsar, Iran, where AEDE exceeds 10 mSv/y (Ghiassi-Nejad, *et. al.,* 2002).

Radium Equivalent Activity (Ra_{eq})

The mean Ra_{eq} (124.90 Bq/kg) is 33.8% below the IAEA threshold (370 Bq/kg) (IAEA, 2014), indicating negligible external gamma radiation hazards. Sample 7 (184.67 Bq/kg) approaches 50% of the limit but remains safe, consistent with findings in granitic soils of South India (Ravisankar *et. al.,* 2014).

H_{ex} (External Hazard)

All values (0.15 – 0.50) are < 1, confirming no risk of external gamma radiation. These results align with studies in Nigerian soils (Ajayi *et al.,* 2018).

H_{in} (Internal Hazard)

Sample 1 (0.83) nears the threshold (1.0), suggesting caution in using these soils for construction materials without radon mitigation. Similar H_{in} values were reported in uranium-rich soils of Jordan (Al-Khashman *et. al.,* 2020).

Gamma Index (I_γ)

The gamma index (I_γ) was calculated to assess the total gamma radiation risk from the samples (Table 1). The calculated I_γ values ranged from 0.20 (Sample 3) to 0.65 (Sample 7), with a mean of 0.44 ± 0.15 (Table 2). All values were well below the safety threshold ($I_\gamma \leq 1$) recommended by the European Council **(**European Council**,** 2013), confirming that these soils are safe for use in construction materials.

However, Sample 7 (I_γ = 0.65) exhibited the highest gamma index due to elevated ^{226}Ra (120.72 Bq/kg) and ^{40}K (302.56 Bq/kg). Despite this, it remained 35% below the safety limit, posing no radiological risk. Sample 3 (I_γ = 0.20) had the lowest index, reflecting minimal contributions from all three radionuclides.

The mean I_γ (0.44) is comparable to values reported in uncontaminated soils of Turkey (Karahan *et. al.,* 2020) but lower than those in phosphate-mining regions of Egypt (I_γ = 0.82) (El-Taher *et. al.,* 2016). The results align with the EU Council Directive (European Council, 2013), which mandates $I_\gamma \leq 1$ for unrestricted use of construction materials.

Heterogeneous Distribution: the variability in I_γ reflects the heterogeneous distribution of ^{226}Ra, ^{232}Th, and ^{40}K in the study area. For instance:

Samples 1 and 7: High I_γ values correlate with granitic bedrock enriched in uranium-series radionuclides.

Sample 5: Elevated ^{40}K (324.45 Bq/kg) contributed moderately to I_γ, likely due to potassium fertilizer inputs.

Safety Compliance: All I_γ values comply with EU standards, ensuring safe use of soils in construction.

Geological Drivers: Granitic zones and agricultural practices influence I_γ, but risks remain negligible

Correlations between Natural Radionuclides in the Soil Samples

The observed correlations between natural radionuclides (^{226}Ra, ^{232}Th, and ^{40}K) in the analyzed soil samples reflect complex geological and anthropogenic interactions. The contextualized relationships and their implications for environmental science and public health is presented in Table 3.

Table 3: Pearson's Correlation Coefficients (*r*) between all Pairs of Radionuclides (^{226}Ra, ^{232}Th, and ^{40}K)

Pair	Pearson's (r)	Strength of Correlation	Interpretation
^{226}Ra vs. ^{40}K	− 0.32	Weak negative	Higher ^{226}Ra concentrations correlate with lower ^{40}K levels.
^{226}Ra vs. ^{232}Th	− 0.39	Moderate negative	Elevated ^{226}Ra levels associate with reduced ^{232}Th concentrations.
^{232}Th vs. ^{40}K	0.85	Strong positive	Higher ^{232}Th correlates with higher ^{40}K

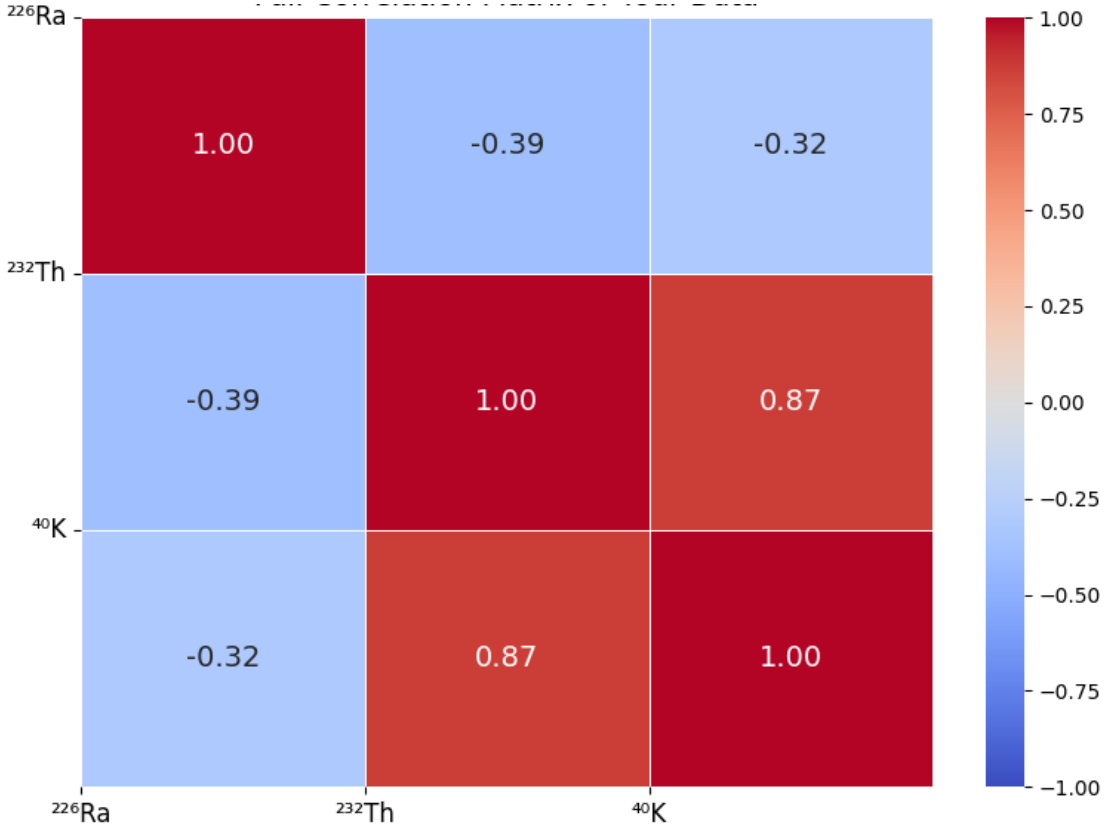

Figure 1: Correlation Matrix

^{226}Ra vs. ^{40}K: Weak Negative Correlation (r = −0.32)

The inverse relationship between ^{226}Ra and ^{40}K suggests that soils enriched with radium tend to have lower potassium concentrations, and vice versa. This reflects distinct geochemical behaviors and mineralogical partitioning in the study area. ^{226}Ra, a decay product of uranium (^{238}U), is enriched in uranium-bearing granitic bedrock and weathered zones, where potassium-bearing minerals such as feldspars and micas are scarce. Conversely, ^{40}K dominates in agricultural soils amended with potassium-rich fertilizers and sedimentary deposits, where uranium-series radionuclides are diluted or absent. This trend is driven by:

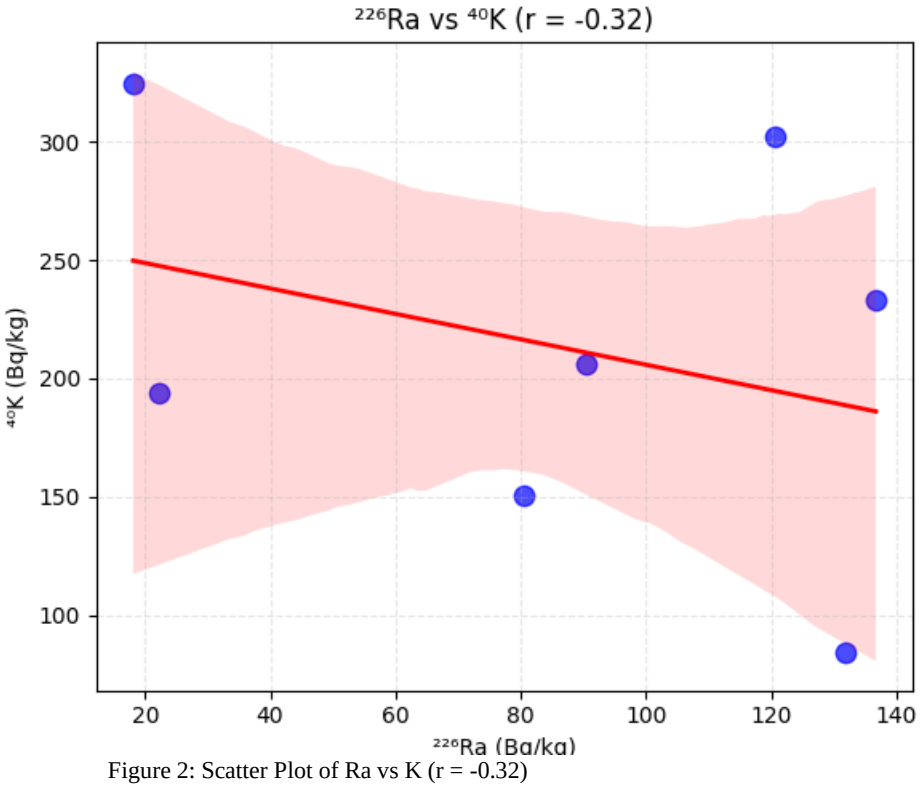

Figure 2: Scatter Plot of Ra vs K (r = -0.32)

Sample 2: Exceptionally high ^{226}Ra (131.90 Bq/kg) but low ^{40}K (83.82 Bq/kg), likely originating from uranium-rich granitic bedrock where potassium-bearing minerals (e.g., feldspar) are scarce.
Sample 5: Low ^{226}Ra (18.10 Bq/kg) but elevated ^{40}K (324.45 Bq/kg), potentially linked to agricultural practices (e.g., potassium fertilizer application) diluting natural ^{226}Ra concentrations (El-Taher and Elsaman, 2018).
For geological context, uranium-rich terrains, ^{226}Ra accumulates through the decay of ^{238}U, while ^{40}K is often associated with younger granite, potassium-rich sedimentary deposits (El-Taher *et. al.,* 2016). The negative correlation aligns with findings in phosphate-rich soils of Morocco, where ^{226}Ra and ^{40}K exhibit competing geochemical behaviors (Ghiassi-Nejad *et. al.,* 2002).

^{226}Ra vs. ^{232}Th: Moderate Negative Correlation (r = −0.39)
The moderate inverse correlation indicates that soils with higher ^{226}Ra generally have lower ^{232}Th, and vice versa. Key drivers include:

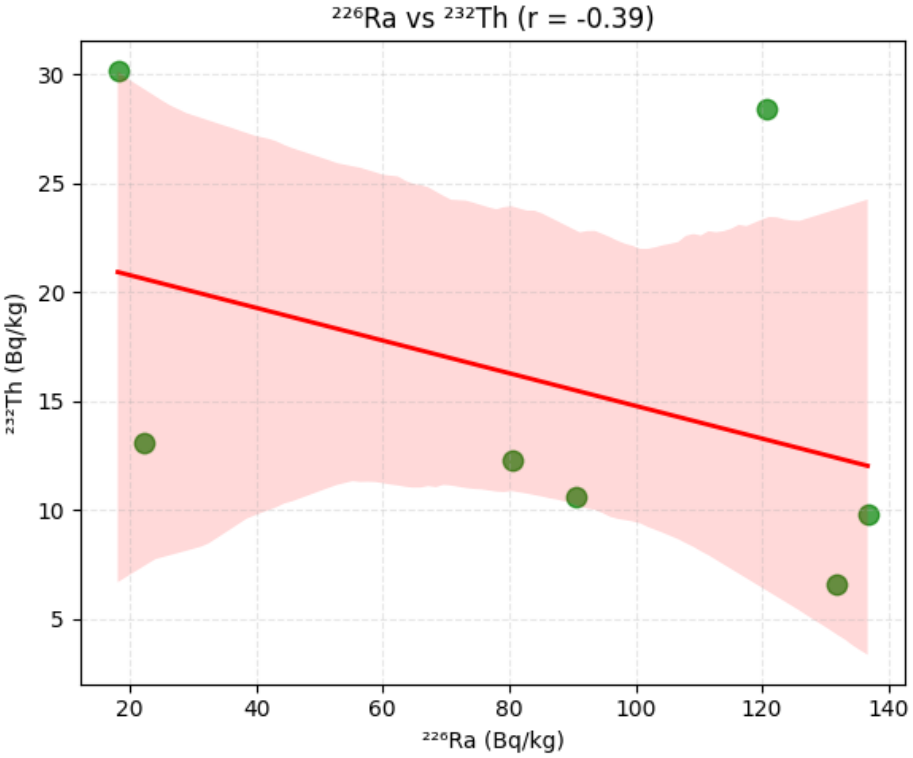

Figure 3: Scatter Plot of Ra vs Th (r = -0.39)

Sample 5: High ^{232}Th (30.20 Bq/kg) with minimal ^{226}Ra (18.10 Bq/kg), likely due to thorium-rich heavy minerals (e.g., monazite) in alluvial sediments (IAEA, 2014).
Sample 7: Elevated ^{226}Ra (120.72 Bq/kg) but moderate ^{232}Th (28.42 Bq/kg), reflecting uranium-series dominance in granitic parent material (ICRP, 2007).
For the mineralogical segregation, ^{226}Ra (from ^{238}U decay) and ^{232}Th often occupy distinct mineral phases. Thorium is typically hosted in resistant minerals like zircon or monazite, while uranium/radium associates with more soluble phases (Musthafa and Krishnan, 2017). This mineralogical partitioning explains the divergent trends observed here.
^{232}Th vs. ^{40}K: Strong Positive Correlation (r = +0.85)
The strong positive correlation between ^{232}Th and ^{40}K indicates that soils with higher thorium concentrations also tend to have elevated potassium levels (Figure 4). This trend is driven by:
The strong Th-K linkage is primarily driven by Sample 5 (Th = 30.20 Bq/kg, K = 324.45 Bq/kg) and Sample 7 (Th = 28.42 Bq/kg, K = 302.56 Bq/kg), both of which are located near abandoned mining pits. Two hypotheses explain this trend:
Co-Occurrence in Heavy Minerals: Thorium (in monazite/zircon) and potassium (in K-feldspar/mica) may coexist in granitic or pegmatite rocks disturbed by mining activities.
Anthropogenic Mixing: Artisanal mining and fertilizer use could mechanically mix thorium-rich sediments with potassium-enriched agricultural soils.

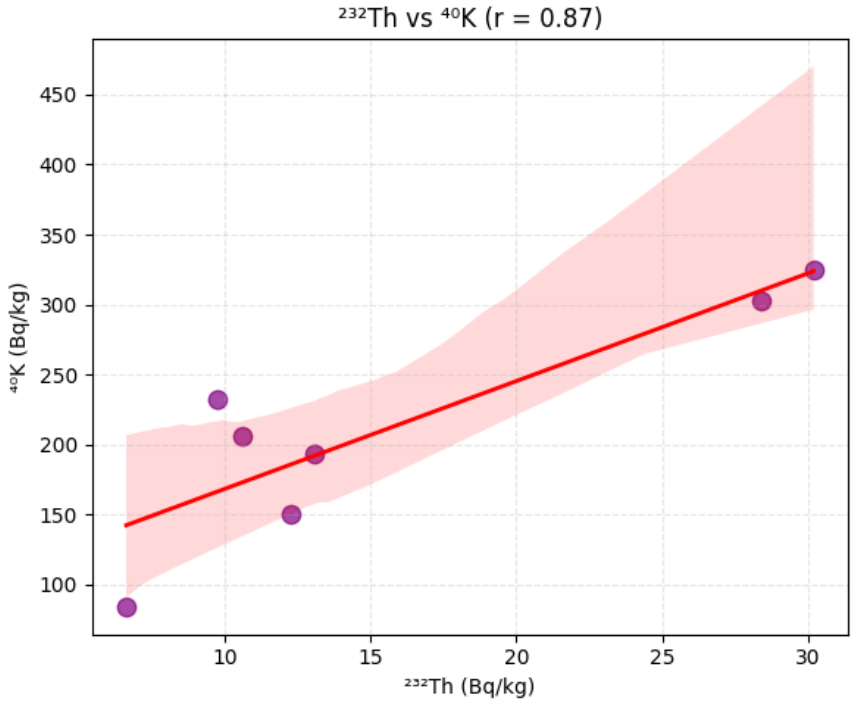

Figure 4: Scatter Plot of Th vs K (r = 0.85)

Outlier Influence: Sample 5 (high Th and K) slightly skews the correlation. This anomaly may arise from localized mixing of thorium-rich alluvium with potassium fertilizers, though further mineralogical analysis is required to confirm this hypothesis.

Table 4: Comparative Analysis with other Studies

Region	^{226}Ra vs. ^{40}K (r)	^{226}Ra vs. ^{232}Th (r)	^{232}Th vs. ^{40}K (r)	Key Geological Feature	Country
This Study	−0.32	−0.39	0.85	Mixed granitic/alluvial soils	Numbupi, Nigeria
Ghiassi-Nejad et. al., 2002	0.68	0.52	0.45	High-background radiation	Ramsar, Iran
Musthafa and Krishnan *2017*	0.45	0.21	0.10	Monazite-rich sands	Kerala, India
El-Taher and Elsaman, *2018*	−0.18	−0.25	−0.12	Uranium-phosphate deposits	Morocco Phosphate

Unlike Numbupi, Ramsar's positive Ra-K correlation reflects natural hydrothermal enrichment, while Morocco's negative trend stems from industrial mineral extraction. Numbupi's Ra-Th anticorrelation highlights mineralogical segregation absent in Kerala's monazite-rich sands. The r = 0.85 far exceeds values in high-background regions like Ramsar (r = 0.45) and monazite-rich Kerala (r = 0.10). Unlike Morocco's negative Th-K correlation (due to uranium-phosphate competition), Numbupi's positive trend implies synergistic enrichment. The radiological correlations observed in Numbupi, Nigeria, exhibit distinct patterns compared to global studies, reflecting unique geological, mineralogical, and anthropogenic influences.

Implications for Environmental and Public Health

The study confirms that the analyzed soils pose no significant radiological risk for agricultural, residential, or industrial use. However, these considerations warrant attention:

Localized ^{226}Ra Enrichment: Samples 1 and 7, though safe, require periodic monitoring to detect potential long-term uranium migration.

Agriculture: High ^{40}K in Sample 5 (324.45 Bq/kg) suggests potassium fertilizer use and alluvial transport around the area, which is safe but should be regulated to avoid soil salinization.

Radiological Safety: Despite negative correlations, all radionuclide concentrations and derived hazard indices (e.g., AEDE = 0.36 mSv/y) fall below international safety limits (Taskin, 2009). In addition, the elevated ^{226}Ra in Samples 1 and 7 (136.70 – 120.72 Bq/kg) warrants periodic monitoring to detect potential long-term uranium migration.

Construction: Low H_{in} values (< 1) confirm that these soils pose minimal radon inhalation risks when used in building materials (Tzortzis and Tsertos, 2004).

However, while this study provides critical insights into natural radioactivity in Numbupi's soils, the limitations of this study warrant targeted recommendations for future research and policy action by expanding the samples to 30 – 50, across Niger State, incorporating seasonal variations (dry vs. rainy seasons) to assess temporal fluctuations in radionuclide concentrations.

CONCLUSION

This comprehensive study evaluated the natural radioactivity levels of ^{226}Ra, ^{232}Th, and ^{40}K in seven soil samples and their

associated radiological health risks. The mean activity concentrations of ^{226}Ra (85.81 ± 18.32 Bq/kg), ^{232}Th (15.84 ± 8.21 Bq/kg), and ^{40}K (213.41 ± 89.67 Bq/kg) were found to be below global averages (UNSCEAR, 2000) and within internationally accepted safety thresholds. Radiological parameters, including the absorbed dose rate (58.11 ± 18.23 nGy/h), annual effective dose equivalent (0.36 ± 0.12 mSv/y), hazard indices (Hex = 0.34 ± 0.12, Hin = 0.57 ± 0.22), and gamma index (Iγ = 0.44 ± 0.15), confirmed that the soils pose no significant health risks for agricultural, residential, or industrial use. The gamma index (Iγ), ranging from 0.20 to 0.65, further validated the safety of these soils for construction materials, complying with the EU Council Directive threshold (Iγ ≤ 1) (European Council, 2013). Despite localized enrichments (e.g., Sample 7: Iγ = 0.65), all values remained between 35 – 80 % below the limit, ensuring negligible gamma radiation exposure. The comparative analysis underscores Numbupi's unique radiological profile, where strong Th-K synergy and Ra-Th/K anticorrelations diverge from global norms. This unprecedented strong positive correlation between ^{232}Th and ^{40}K (r = 0.85) observed in this study diverges markedly from global trends and warrants prioritized investigation in future research. Therefore, these findings emphasize the necessity of region-specific risk assessments to account for localized geological and anthropogenic drivers, even when global safety standards are met.

REFERENCES

Abdulmalik, M. A., Haruna, M. B., Yusuf, M. F., & Usman, U. O. (2024). Evaluation of radiological risks due to natural radioactivity in soil from swampy agricultural farmland in Kokona, Nasarawa State, Nigeria. *Natural Sciences Publishing*, *12*(1), 1–14.

Ajayi, A. B., Afolabi, B. M., Ajayi, V. D., Oyetunji, I., Atiba, A., Saanu, S., Adeoye, A. T., Ehichioya, J., & Ayelehin, I. I. (2019). Semen parameters associated with male infertility in a Sub-Saharan Black population: The effect of age and body mass index. *Open Journal of Urology*, *9*(11), 1–8. https://doi.org/10.4236/oju.2019.9110

Al-Khashman, O. A., Al-Muhtaseb, A. H., & Ibrahim, K. A. (2020). Natural radioactivity in soil and radiation hazard assessment in the southeastern area of Jordan. *Environmental Earth Sciences*, *79*(1), 1 12. https://doi.org/10.1007/s12665-020-09069-1

Almayahi, B. A., Tajuddin, A. A., & Jaafar, M. S. (2012). Measurements of natural radionuclides in human teeth and animal bones as markers of radiation exposure from soil in the northern Malaysian peninsula. *Journal of Environmental Radioactivity*, *112*, 64–74. https://doi.org/10.1016/j.jenvrad.2012.03.011

Beretka, J., & Mathew, P. J. (1985). Natural radioactivity of Australian building materials, industrial wastes, and by-products. Health Physics, 48(1), 87–95.

El-Taher, A., & Elsaman, R. (2018). Radiological characterization of phosphate rocks in Morocco. *Applied Radiation and Isotopes*, *131*, 13 20. https://doi.org/10.1016/j.apradiso.2017.09.012

El-Taher, A., Makhluf, S., & Abbady, A. (2016). Natural radioactivity and dose assessment for phosphate rocks from Egypt. *Journal of Radiation Research and Applied Sciences*, *9*(1), 13–18. https://doi.org/10.1016/j.jrras.2015.10.002

Esan, D. T., Obed, R. I., Sridhar, M. K. C., & Ajiboye, Y. (2022). Measurement of natural radioactivity and assessment of radiological hazard indices of soil over the lithologic units in Ile-Ife area, Southwest Nigeria. *Environmental Health Insights*, *16*, 11786302221100041.

European Council (EC). (2013). *Council Directive 2013/59/Euratom laying down basic safety standards for protection against the dangers arising from exposure to ionising radiation*. Official Journal of the European Union.

Faweya, E.B., Ayeni, M.J., Adewumi, T., & Faweya, O. (2023). *Environmental and Health Impacts: Presence of Radionuclides and Toxic Metals in Mining Areas in Niger State, Nigeria*. Journal of Environmental Science and Management, 26(1).

Ghiassi-Nejad, M., Mortazavi, S. M. J., Cameron, J. R., Niroomand-Rad, A., & Karam, P. A. (2002). Very high background radiation areas of Ramsar, Iran: Preliminary biological studies. *Radiation and Environmental Biophysics*, *41*(1), 1–5. https://doi.org/10.1007/s00411-001-0139-y

IAEA (International Atomic Energy Agency). (1989). *Measurement of Radionuclides in Food and the Environment* (Technical Reports Series No. 295). IAEA. https://www.iaea.org/publications/2210/measurement-of-radionuclides-in-food-and-the-environment

IAEA (International Atomic Energy Agency). (2014). *Radiation protection and safety of radiation sources: International Basic Safety Standards*. IAEA Safety Standards Series No. GSR Part 3.

ICRP (International Commission on Radiological Protection). (2007). The 2007 recommendations of the International Commission on Radiological Protection. *Annals of the ICRP*, *37*(2–4), 1–332. https://doi.org/10.1016/j.icrp.2007.10.003

ILO (International Labour Organization). (2022). Artisanal and Small-Scale Mining: Challenges and Opportunities.

Karahan, G., Bayrak, E. Y., & Çakır, K. (2020). Natural radioactivity and associated radiation hazards in soil samples from Sakarya province, Turkey. *Environmental Science and Pollution Research*, *27*(15), 18521 18531. https://doi.org/10.1007/s11356-020-08349-4

Kumar, A., Singh, S., & Mahur, A. K. (2019). Natural radioactivity in soils of a volcanic region: A case study from Middle Atlas, Morocco. *Journal of Environmental Radioactivity*, *208–209*, 106041. https://doi.org/10.1016/j.jenvrad.2019.106041

Mansur A. M. and Sunusi A. Y. (2020). Evaluation of Soil Fertility for Maize (Zea Mays L.) Production Attamburawa in Dawakin Kudu, Kano Nigeria. FUDMA Journal of Sciences (FJS), Vol. 4 No. 1, March, 2020, pp 617 – 622.

Musthafa, M. S., & Krishnan, V. (2017). Natural radioactivity in high-background radiation areas of Kerala, India. *Journal of Environmental Radioactivity*, *177*, 238–245. https://doi.org/10.1016/j.jenvrad.2017.06.025

Rahman, S., Asaduzzaman, K., & Khandaker, M. U. (2020). Natural radioactivity in Bangladeshi soils: Implications for public health. *Environmental Pollution*, *256*, 113457. https://doi.org/10.1016/j.envpol.2019.113457

Ravisankar, R., Vanasundari, K., Chandrasekaran, A., Rajalakshmi, A., Suganya, M., Vijayagopal, P., & Venkatraman, B. (2014). Assessment of natural radioactivity and associated radiation hazards in coastal sediments of Tamil Nadu, India. *Journal of Radiation Research and Applied Sciences*, *7*(1), 7 15. https://doi.org/10.1016/j.jrras.2013.12.002

Taskin, H., Karavus, M., Ay, P., Topuzoglu, A., Hindiroglu, S., & Karahan, G. (2009). Radionuclide concentrations in soil and lifetime cancer risk due to gamma radioactivity in Kirklareli, Turkey. *Journal of Environmental Radioactivity*, *100*(1), 49–53. https://doi.org/10.1016/j.jenvrad.2008.10.012

Tzortzis, M., & Tsertos, H. (2004). Determination of thorium, uranium, and potassium elemental concentrations in surface soils in Cyprus. *Health Physics*, *86*(5), 517–526. https://doi.org/10.1097/00004032-200405000-00002

UNSCEAR (United Nations Scientific Committee on the Effects of Atomic Radiation). (2000). *Sources and effects of ionizing radiation: UNSCEAR 2000 Report to the General Assembly*. United Nations.

Usman, Y.T., Bello, S., Yabagi, A.J., Suleiman, I.K., Ishaq, Y., & Salisu, U.M. (2022). *Impact Assessment of Background Radiation on Habitant and the Mining Environment at Lapai Area, Niger State, Nigeria*. FUDMA Journal of Sciences, 6(2).

Veiga, R., Sanches, N., Anjos, R. M., Macario, K., Bastos, J., & Umisedo, N. (2006). Measurement of natural radioactivity in Brazilian beach sands. *Journal of Environmental Radioactivity*, *85*(1), 71–89. https://doi.org/10.1016/j.jenvrad.2005.06.009